

03,05,07

Magnetic susceptibility of hybrid SiC/Si structures synthesized by coordinated atomic substitution method

© S.A. Kukushkin¹, N.I. Rul'^{1,2,3}, E.V. Ubyivovk^{1,4}, A.V. Osipov¹, V.V. Romanov², N.T. Bagraev^{1,3}

¹ Institute for Problems in Mechanical Engineering of the Russian Academy of Sciences,
St. Petersburg, Russia

² Peter the Great Saint-Petersburg Polytechnic University,
St. Petersburg, Russia

³ Ioffe Institute,
St. Petersburg, Russia

⁴ St. Petersburg State University,
St. Petersburg, Russia

E-mail: sergey.a.kukushkin@gmail.com

Received March 24, 2025

Revised April 25, 2025

Accepted April 25, 2025

The static magnetic susceptibility of SiC/Si hybrid structures grown by the method of coordinated substitution of atoms (MCSA method) at different synthesis times has been measured. The static susceptibility of the samples under study was carried out by using the Faraday method on the Faraday Balance setup based on the MGD 312 FG spectrometer. The results showed that all SiC/Si structures, regardless of the time of their synthesis, are diamagnets ($\chi < 0$), and the absolute of their magnetic susceptibility, measured at room temperature, is more than three orders of magnitude higher than the absolute values of the magnetic susceptibility of both silicon and silicon carbide. As a result of the structural studies of both the SiC layer it was found that the main contribution to the diamagnetism of the hybrid structure is made by the transition layer at the SiC/Si interface. It was found that this layer consists of twin ordered layers located parallel to the interface boundary in the (111) plane with a period of 0.252 nm with a triple periodicity, i.e. with an interval of 0.756 nm. Quantum mechanical calculations have shown that these twinned ordered layers contain ordered ensembles of silicon vacancies located along the $\langle 1\bar{1}0 \rangle$ direction.

Keywords: magnetic susceptibility, diamagnetism, silicon carbide on silicon, silicon vacancies, terahertz radiation, nanostructures.

DOI: 10.61011/PSS.2025.04.61262.55-25

1. Introduction

This study is a continuation of the papers [1–3]. The processes of crystal structure evolution and surface properties of single-crystalline Si during its chemical transformation into an epitaxial SiC layer were studied in these papers. Si was chemically transformed into SiC by the method of coordinated substitution of atoms (MCSA) developed in a series of works, the main provisions of which are summarized in a number of reviews [4,5]. MCSA method is based on the reaction of the interaction of gaseous carbon monoxide (CO) with the surface of single-crystalline silicon at a certain temperature, pressure, and flow rate of CO. One of the silicon atoms is removed as a result of this reaction, volatilizing with the SiO molecule, and the other, which is in the Si crystal lattice, combines with carbon CO. In doing so, a vacancy is formed in the silicon cell. A distinctive feature of this reaction, which allows the growth of highly refined silicon carbide layers on the silicon surface, is that it proceeds in three stages separated by time, unlike the reactions used in classical methods of growing of SiC on Si [6–8].

A detailed description of the changes occurring during the formation of the SiC/Si structure and the associated significant changes in a number of physical properties of SiC/Si hybrid heterostructures can be found in Refs. [1–3]. They can be briefly described as follows:

- on Si substrates of *p*- and *n*-types of conductivity, the processes of SiC formation proceed in a similar manner; there are only slight differences in the kinetics of the chemical transformation of Si into SiC;
- in SiC films grown on both Si(111) substrates of *p*-type of conductivity and Si(111) substrates of *n*-type of conductivity, only compressive elastic strains are formed during the synthesis process; however, the films synthesized on Si(111) substrates of *p*-type of conductivity are elastically more compressive compared to those synthesized on Si(111) substrates of *n*-type of conductivity;
- elastic strains in the SiC film are significantly dependent on SiC synthesis time, having a maximum value at the beginning of synthesis (1 min of synthesis) and completely relaxing by 40th minute of synthesis;
- significant changes are undergone in the optical properties of the films, in particular, there are significant changes in the photoluminescence and ellipsometric spectra.

Significant changes in the microstructure of SiC/Si samples were also confirmed by scanning electron microscopy (SEM).

SiC/Si(111) hybrid structures grown by the coordinated atom substitution method were found to be diamagnetic in Ref. [9]. Moreover, the SiC/Si structures, possess significantly larger absolute values of magnetic susceptibility $\chi(T, H)$, both compared to the magnetic susceptibilities of silicon $\chi(T, H) = -0.228 \cdot 10^{-6} \text{ cm}^3/\text{g}$ at 300 K [10] and silicon carbide $\chi(T, H) = -0.265 \cdot 10^{-6} \text{ cm}^3/\text{g}$ at 300 K [10]. Moreover, magnetic susceptibility hysteresis was found in SiC/Si samples in weak magnetic fields at room temperature in Ref. [9], which is not observed in either silicon or silicon carbide.

Therefore, the aim of this paper was to measure the static magnetic susceptibility of SiC/Si structures and investigate it as a function of synthesis time of SiC/Si hybrid structures. In addition to the data we have previously obtained by scanning electron microscope in Ref. [3] along with measurements of the magnetic susceptibility of the SiC/Si structure, we analyzed in this paper both the SiC films themselves and their interfaces by high-resolution transmission electron microscopy (HR TEM).

2. Materials and methods

Magnetic susceptibility measurements were performed on the same samples of SiC/Si hybrid structures whose structure evolution was investigated and described in Ref. [3]. The SiC films studied in Ref. [3], were grown on the surface of facets (111) of Si wafer of *p*- and *n*-type of conductivity over the following times: 1; 3; 5; and 40 min. The method for synthesizing such structures is described in Ref. [3]. Here, we only briefly describe the main steps of SiC/Si synthesis. Before growing of SiC the surface of Si wafers was cleaned from possible organic impurities, foreign micro-particles, metal ions and anions. A layer of silicon oxide was removed from the surface of Si wafers, and then the surface was passivated with hydrogen as required to obtain a highly refined SiC layer on Si according to the technique described in Ref. [11]. SiC was grown at 1270 °C in an atmosphere of a mixture of CO and SiH₄ gases with flow rates of $Q_{\text{CO}} = 12 \text{ ml/min}$ and $Q_{\text{SiH}_4} = 3 \text{ ml/min}$. The total gas mixture pressure of CO and SiH₄ during growth was $P_{\text{CO+SiH}_4} = 360 \text{ Ra}$. The synthesis process at each of the time intervals (1, 3, 5, 40 min) was conducted simultaneously on substrates of both *p*-type and *n*-type of conductivity, i.e., substrates were kept in the reactor under the same growth conditions.

The static magnetic susceptibility of the samples was measured using the Faraday method. This method, used to study the magnetic properties of weakly magnetic materials, is based on the use of special scales with electromagnetic compensation. This method is based on measuring the interaction force of a sample of mass *m* with an inhomogeneous external magnetic field. The relationship between the value

of the specific static magnetic susceptibility $\chi(T, H)$ and the measured force $F(T, H)$ acting on a sample placed in a magnetic field gradient is defined by the expression

$$\chi(T, H) = F(T, H)/(mH dH/dz).$$

The external magnetic field gradient dH/dz is created by the special shape of the magnet pole tips. The shape of the pole tips ensures that the value of the product $H dH/dz$ remains constant in the entire volume occupied by the sample. For measurements, the samples under study were placed in a quartz cup connected to the scales by a quartz suspension. The force $F(T, H)$ acting on the sample was found as the difference of the magnetic field interaction force with the sample placed in the cup and the force acting on the empty cup under the same experimental conditions.

The experimental setup was calibrated using a reference sample, magnetically pure indium phosphide with a magnetic susceptibility of $\chi(T, H) = -0.313 \cdot 10^{-6} \text{ cm}^3/\text{g}$.

Measurements were performed on a Faraday Balance facility based on the MGD 312 FG, FG spectrometer at room temperature in the range of magnetic fields of 1.5–4 kOe. The sweep of the external magnetic field in the experiment was performed with steps 5, 10, and 200 Oe. The microstructure of the SiC/Si layers was investigated by high-resolution transmission electron microscopy (HR TEM).

3. Experimental results

For convenience in presenting the results, we denote the SiC/Si samples as follows. The chemical symbols denote the chemical structure of the sample, the numbers denote the synthesis time in minutes, and the Latin letters *p* and *n* respectively denote the conductivity type of the silicon substrate. For example, the number SiC/Si-1*p* means that the SiC layer was grown on Si of *p*-type of conductivity and its synthesis continued for 1 min.

Figure 1 shows the results of magnetic susceptibility measurements of SiC/Si structures synthesized during: 1, 3, 5 and 40 min.

Figure 1 shows that the magnetic susceptibility behavior of SiC samples grown on Si of *p*- and *n*-types of conductivity are significantly different from each other, and the obtained dependences have a very curious feature. First, the magnetic susceptibility of all, without exception, SiC/Si samples is negative, i.e. all SiC/Si samples are diamagnetic. Second, the functional dependences of the specific magnetic susceptibility of SiC samples grown on Si of *p*- and *n*-types of conductivity are almost mirror images of each other. The maximum, absolute value of magnetic susceptibility is possessed by the SiC/Si sample synthesized on a Si substrate of *p*-type of conductivity for 40 min. The magnetic susceptibility of a similar sample but synthesized on a Si substrate of *n*-type of conductivity is half as large. An inversion of the obtained dependencies is observed at low synthesis times of SiC samples grown on Si of *p*- and *n*-type of conductivity. The absolute susceptibility value of the SiC sample grown

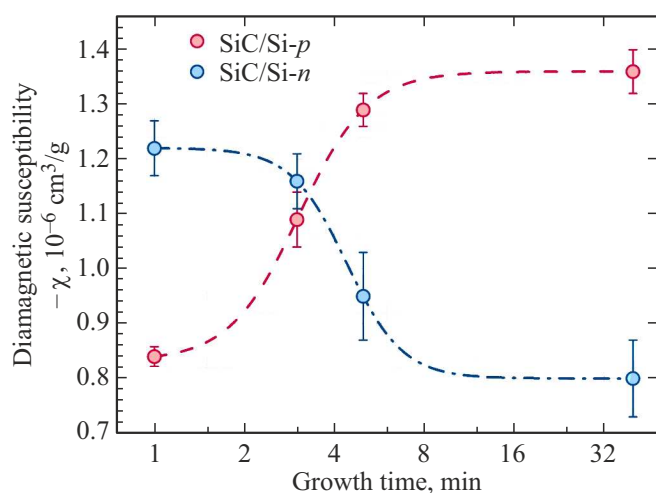


Figure 1. The dependences of the magnetic susceptibility of SiC/Si samples grown on Si(111) surface on the synthesis time; on the vertical axis magnetic susceptibility values taken with the opposite sign are plotted; on the horizontal axis — values of synthesis time; dots in the figure indicate the synthesis times of the samples.

on Si of *n*-type of conductivity for 1 min is greater than the SiC sample synthesized on Si of *p*-type of conductivity for the same time. SiC samples obtained on Si substrates of *p*- and *n*-types of conductivity during 3 min synthesis have close magnetic susceptibility values. The magnetic susceptibility of the SiC sample grown on Si substrate of *p*-type smoothly increases its diamagnetism with the increase of synthesis time, tending to saturation. In contrast, the diamagnetism of the SiC sample grown on Si substrate of *n*-type decreases and saturates after forty minutes of synthesis. As already mentioned, the diamagnetism of the studied samples is characterized by much larger values of magnetic susceptibility than silicon and silicon carbide.

The magnetic susceptibilities of SiC/Si hybrid structures are comparable in order of magnitude to magnetic susceptibilities of polycrystalline graphite with magnetic susceptibility of $\chi(T, H) = 3.0 \cdot 10^{-6} \text{ cm}^3/\text{g}$ at 289 K [10,12]. It should be noted that we characterized the diamagnetism of the SiC layer by averaging the magnetic susceptibility value over its mass. However, if the main diamagnetic contribution is made only by a small part of the layer formed in a certain way, its magnetism will be described by a significantly larger value of the magnetic susceptibility.

4. Discussion and analysis of results

The experimental data obtained are very interesting from two points of view. First, the following legitimate question arises. What is the reason for such a strong diamagnetic response of structures to an external magnetic field. Second, the nontrivial dependence of the magnetic susceptibility on the growth time of hybrid SiC/Si structures is surprising.

The analysis of the time evolution processes conducted in Ref. [3] showed that differences in the kinetics of the formation and growth are still observed during the transformation of Si into SiC on Si substrates of *p*-type and on Si substrates of *n*-type although proceeding in a similar manner. Thus X-ray diffraction [2] studies have shown that there are no elastic deformations at all synthesis stages in SiC films grown on Si substrates of *n*-type of conductivity. In contrast, SiC films synthesized on Si substrates of *p*-type of conductivity during 1 min are elastically compressed. The elastic stresses also completely relax in SiC structures grown on Si substrates of *p*-type of conductivity with the increase of the synthesis time. At the same time, the pore density (based on scanning microscopy data in Ref. [3]), in the Si substrate of *p*-type, exceeds the pore density in the *n*-type substrate in case of SiC synthesis during 40 min. However, all the basic properties of SiC/Si films, namely optical (measured by ellipsometry, Raman spectroscopy, and photoluminescence spectra), surface properties, i.e. reconstruction, layer thicknesses, and pore densities in SiC/Si structures, generally change symbate with each other.

It should be noted that if SiC films were grown on Si using a standard method, such as the CVD [6–8], then the growth process would increase the thickness of the films, while the film properties themselves remain unchanged. Everything is different in the case of SiC grown on Si by the method of coordinated substitution of atoms (MCSA). A solid SiC layer is formed in less than minute in case of growth by this method. Further synthesis of the layers, leads only to changes in the composition and structure of the SiC/Si interface and the structure of the diffusion zone in the silicon substrate. It is the structure of the SiC/Si boundary that, in our opinion, determines the unusual behavior of the specific magnetic susceptibility dependences shown in Figure 1. It was found in Refs. [13,14] that a thin intermediate layer with dielectric permittivity corresponding to a half-metal is formed at the 3C-SiC(111)/Si(111) interface. It was also suggested in Refs. [13,14] that so-called partial dislocations are formed at the SiC/Si interface, leading to the formation of stacking faults with interlayers of densely stacked hexagonal phases (4H-SiC and 6H-SiC) located in the main phase of cubic silicon carbide [3].

The magnetic susceptibility measurement data and the results obtained in Ref. [9] led us to realize the need for a more thorough analysis of the SiC/Si interface by high-resolution transmission electron microscopy (HR TEM). The same SiC/Si samples with the numbers SiC/Si-*T_p* and SiC/Si-*T_n*, in which the letter T denotes the synthesis time of the samples, were used for structure studies by TEM. This paper for saving space presents the HR TEM images of the layer structure and electron diffraction images of the interface of SiC/Si hybrid structures grown at times at which the most significant changes in magnetic susceptibility are observed, i.e. at 1, 3, and 40 min. Thin layers were prepared from these samples, across the growth axis in the $\langle 111 \rangle$ direction, for further investigation by TEM techniques.

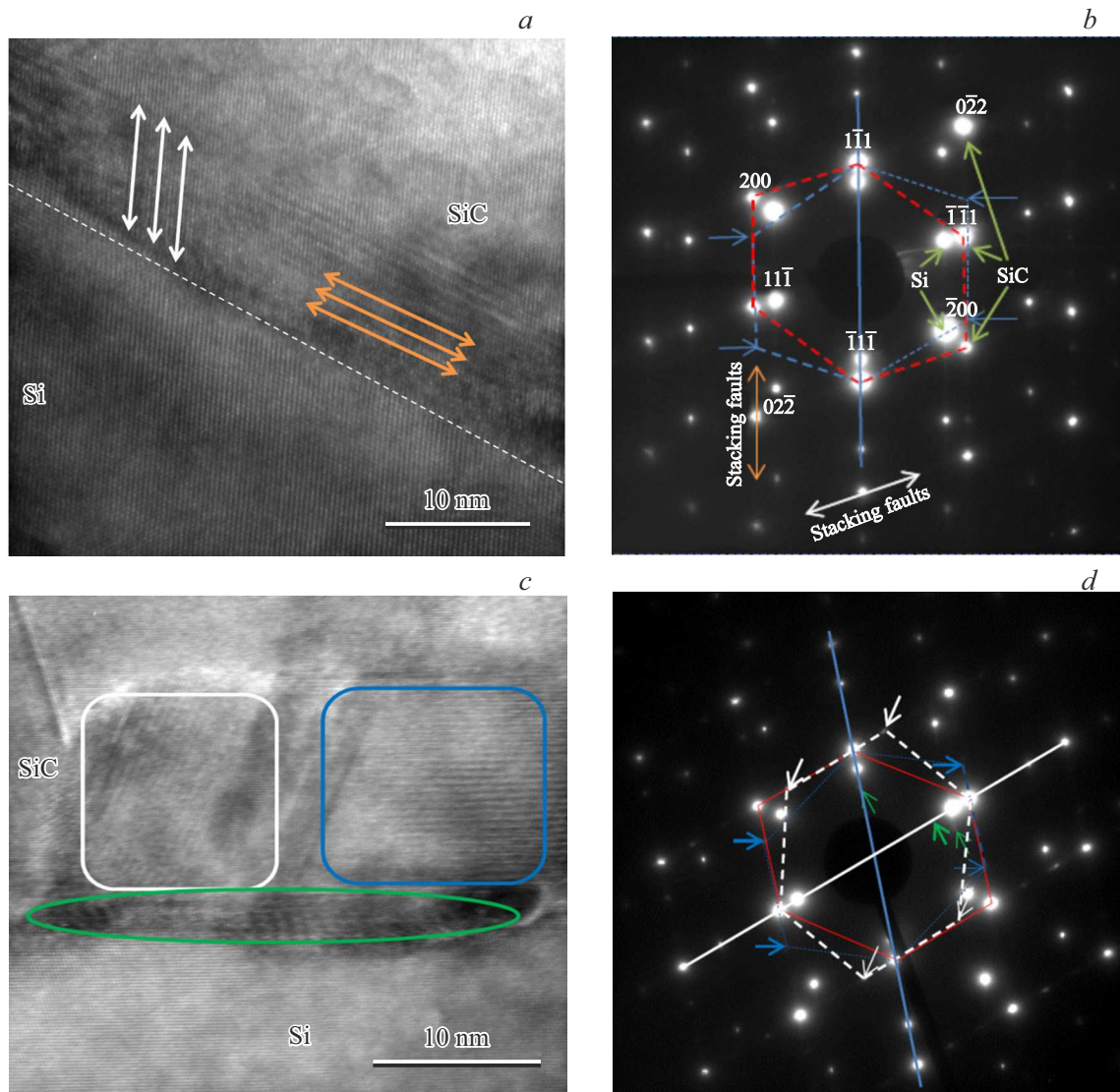


Figure 2. HR TEM cross-section and electron diffraction patterns of the interfacial interface of SiC/Si-1*n* and SiC/Si-1*p* samples; (a) — sample of SiC/Si-1*n*, (b) — selected area electron diffraction (SAED) patterns recorded from a section of the interface of this substrate; (c) — sample SiC/Si-1*p*, (d) — selected area electron diffraction (SAED) patterns recorded from a section of the interface of a given substrate.

Figures 2–4 shows the HR TEM images of the layer structure and electron diffraction images of the interface of SiC/Si hybrid structures grown on substrates of *n*- and *p*-type of conductivity for 1, 3, and 40 min.

The white dashed line in Figure 2, *a* is the line showing the interface between Si and the twin transition layer SiC; orange arrows indicate stacking faults running parallel to the SiC/Si boundary; white arrows indicate stacking faults lying at an angle of 54.75° to the SiC/Si boundary. Twinning reflections from „triple periodicity“ are indicated by blue arrows in Figure 2, *b*; the twinning axis is indicated by a blue line; red dashed lines are drawn along the reflexes of the main SiC matrix; blue dashed lines mark the twinning; Si and SiC reflexes are indicated by green arrows, respectively. Light bands of weak intensity connecting the

main reflexes in two directions are tractions caused by stacking faults; orange arrows indicate tractions parallel to the SiC/Si boundary (corresponding to the orange arrows in Figure 2, *a*); white arrows indicate the streaks oriented at the angle of 54.75° (corresponding to the white arrows in Figure 2, *a*). The white region in Figure 2, *c* highlights the „triple periodicity“ stacking faults located in the SiC layer and oriented at an angle of 54.75° to the SiC/Si boundary; the blue region highlights the „triple periodicity“ stacking faults located in the SiC layer and oriented parallel to the SiC/Si boundary; the green region highlights the Moire pattern formed by superposition of two disoriented Si crystal lattices; the green arrows in the Figure 2, *d* indicate additional reflections formed around the main Si reflections from superposition of two Si lattices; low-

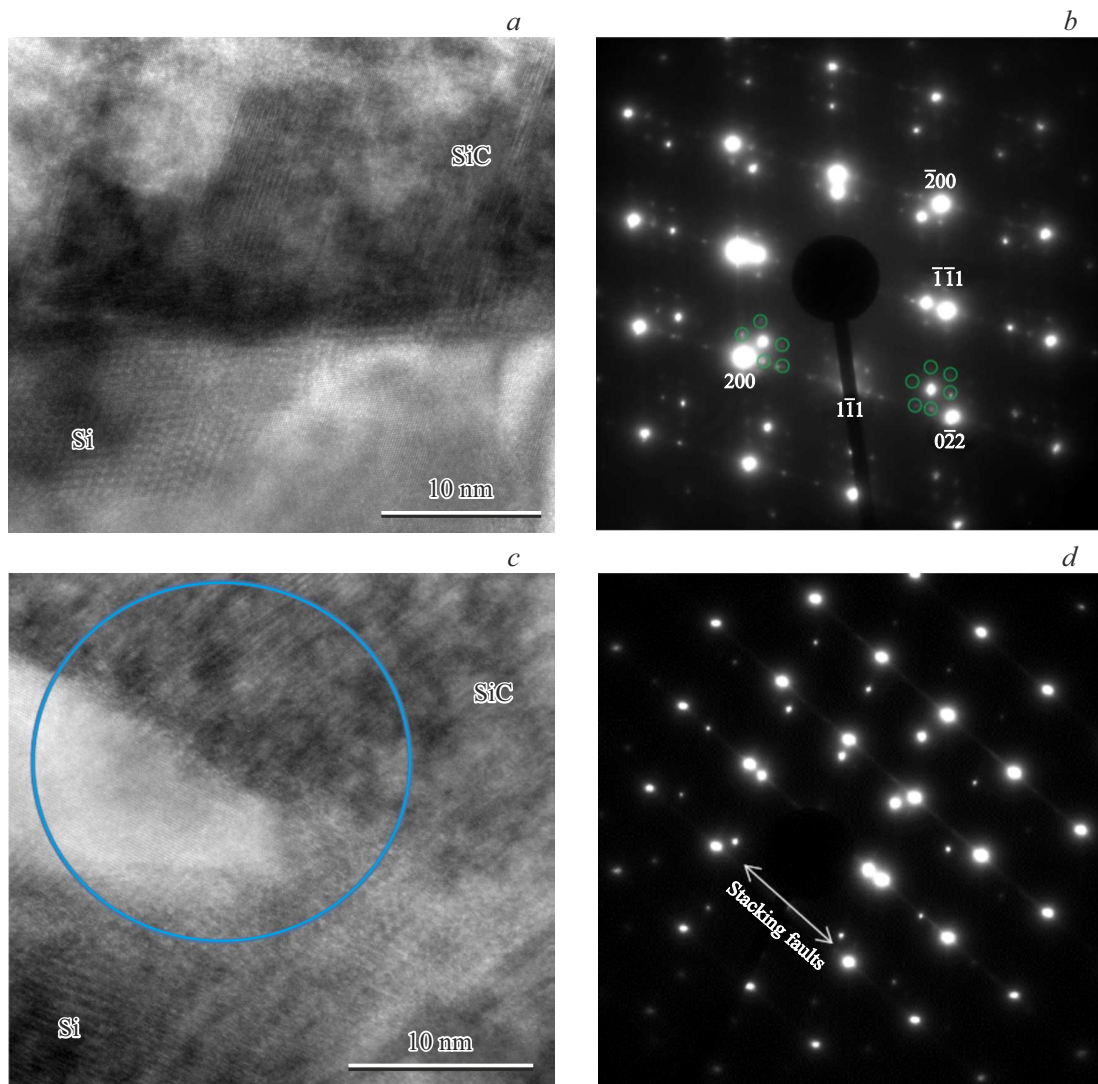


Figure 3. HR TEM cross-section images and selected area electron diffraction (SAED) patterns recorded from patterns of the interfacial interface of the SiC/Si-3*n* and SiC/Si-3*p* samples; (a) — sample SiC/Si-3*n*, (b) — selected area electron diffraction (SAED) patterns recorded from a section of the interface of this substrate; (c) — sample SiC/Si-3*p*, (d) — selected area electron diffraction (SAED) patterns recorded from a section of the interface of a given substrate; the green circles in Figure 3, *b* separate the main Si reflections, from the brighter reflections of the „double diffraction“.

intensity reflections from twinning of the main matrix are shown by white and blue arrows, respectively.

The electron diffraction pattern on Figure 3, *d* is acquired using the „selective aperture“ from the region highlighted by the blue circle in the TEM image of Figure 3, *c*; the white double arrow indicates streaks along the SiC reflexes located in one direction only, which correspond to stacking faults oriented at an angle of 54.75° .

The stacking faults in the interfacial boundary region are clearly visible on the HR TEM images of the end chips of the interface of SiC/Si sample SiC/Si-1*n* shown in Figures 2–4. Electron diffraction shows the presence of cubic phase of 3C-SiC in the carbide layer, in addition to the main reflexes there are less intense reflexes from twins of phase of 3C-SiC, and also there is a system of streaks

in two directions (light bands of weak intensity connecting the main reflexes), corresponding to stacking faults. The triple periodicity is observed in the form of bands running parallel to the interface boundary in the SiC layer closer to the substrate boundary. In the electron diffraction pattern, in addition to the primary SiC reflections, twin reflections from „triple periodicity“ are visible (marked by blue arrows; the twinning axis is indicated by a blue line). Red dashed lines are drawn along the reflections of the main SiC matrix, while the twin is marked by a blue dashed line. In addition to reflexes from twins in SiC, we observe streaks (light bands of weak intensity connecting the main reflexes) in two directions, such streaks are caused by stacking faults oriented parallel to the SiC/Si boundary). They are indicated

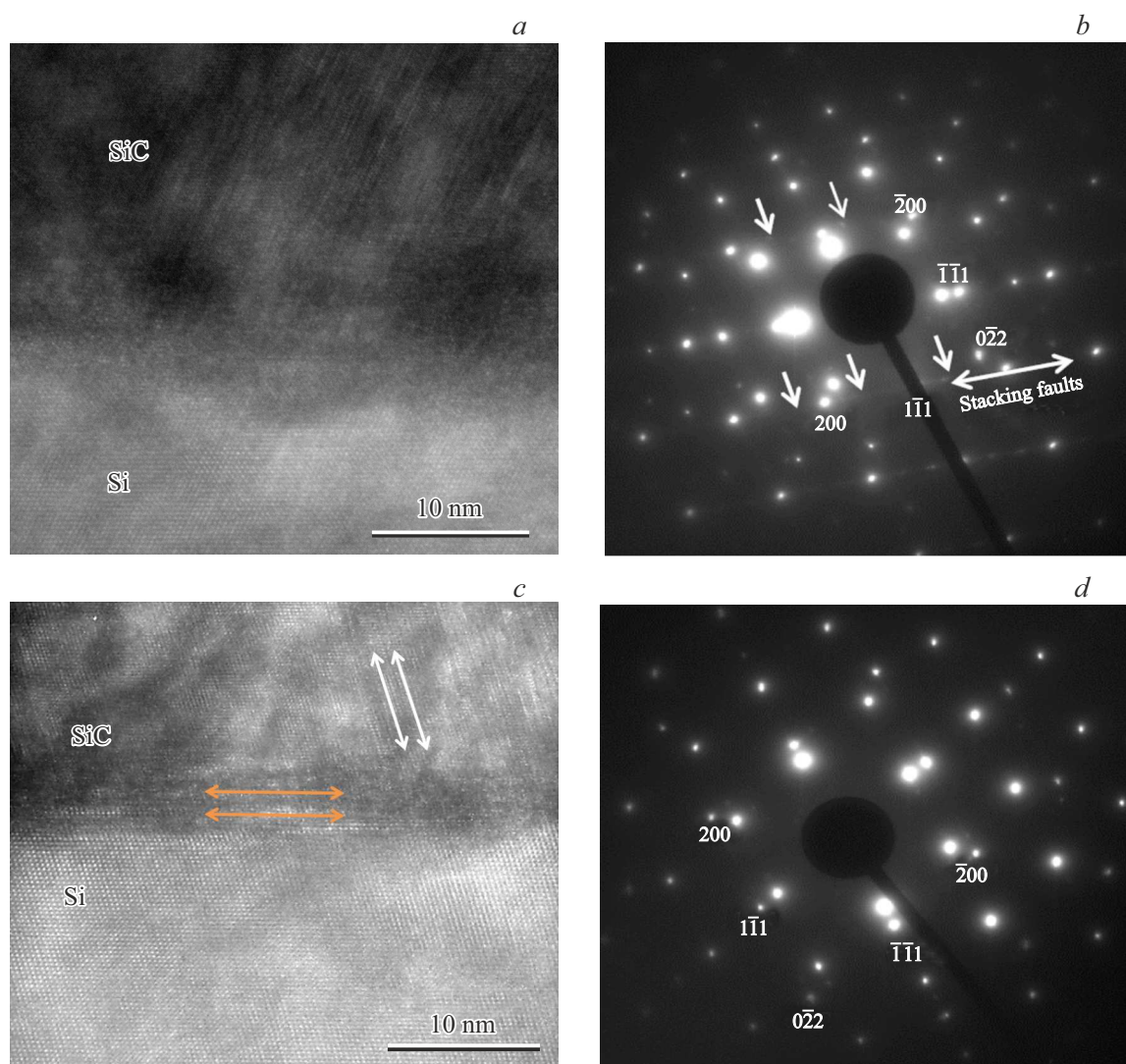


Figure 4. HR TEM cross-section images and electron diffraction patterns of the interphase boundary of the SiC/Si-40 n and SiC/Si-40 p samples; (a) — SiC/Si-40 n sample, (b) — selected area electron diffraction (SAED) patterns recorded from a section of the interface of this substrate; (c) — sample SiC/Si-40 p , (d) — selected area electron diffraction (SAED) patterns recorded from a section of the interface of a given substrate; white arrows (Figure 4, (b)) indicate the presence of stacking faults oriented at an angle of 54.75° to the interface. Orange arrows indicate stacking faults oriented parallel to the SiC/Si interface; white arrows indicate stacking faults oriented at an angle of 54.75° to the SiC/Si interface.

by orange arrows. Streaks oriented at an angle of 54.75° are indicated by white arrows.

The pattern of the interface structure shown in these figures is similar to the pattern, of the 3C-SiC layer structure, given in Ref. [15]. Epitaxial films of cubic 3C-SiC, which was grown by molecular beam epitaxy (MBE) on the surface of hexagonal single crystal 6H-SiC, have been studied by HR TEM. The authors of the paper [15] found that along the regions of the 3C-SiC polytype, possessing a crystal structure, regions exhibiting triple periodicity with an interval of 0.756 nm are observed. This distance is half the constant „ c “ of the lattice of 6H-structure. After analyzing the microdiffraction patterns, the authors of the paper [15] concluded that these regions are nothing but the overlapping

regions of the twins of the polytype 3C-SiC. This overlap results in the formation of layers with a period of 0.252 nm, with a repetition of this structure every three layers. The distance between layer repetitions is 0.756 nm. A similar structure is formed in the interface zone as follows from the pattern of microphotography shown in Figure 2, *b* and in our case. The microdiffraction image shown in Figure 2, *b* and taken from this area also indicates this and, therefore, can be described using the model of overlapping twin 3C-SiC phases with triple periodicity [15]. In our case, the triple-periodicity sites are located along the 3C-SiC/Si interface, while in the case of the growth of 3C-SiC on 6H-SiC by MBE method [15], these regions are located inside the 3C-SiC layer and are bounded from the sides by

defects of another type. In the case of SiC growth on Si by the method of coordinated atom substitution, another structure is formed besides the structure of twins with triple periodicity formed at the interface inside the interface layer. This structure, as can be clearly seen in Figure 2, *a*, is oriented at an angle of 54.75° . This Moire pattern, indicates that the SiC layer contains stacking faults located in two directions $\langle 100 \rangle$. Inside the interface layer (Figure 2, *a*), the formation of these defects can be seen. They have just begun to form and, as will be seen later, at longer times these defects will sprout into the SiC layer.

Let us now turn to Figure 2, *c* and Figure 2, *d*. These figures show a TEM image of the SiC/Si interface and the corresponding electron microdiffraction image from this interface of the SiC/Si-1*p* sample.

It is evident from Figure 2 that the structure of the SiC/Si interface of the SiC/Si-1*p* sample is fundamentally different from the structure of the SiC/Si interface of SiC/Si-1*n* sample (Figure 2, *a*). There is no Moire pattern in the interface area in SiC/Si-1*p* sample. However, twins began to appear in the 3C-SiC layer itself away from the SiC/Si interface. Both twins parallel to the interface, along the interface, and twins located at an angle of 54.75° in the $\langle 100 \rangle$ directions are present in layer 3C-SiC. In difference to the twins in the SiC/Si-1*n* sample, the twins in the SiC/Si-1*p* sample are poorly formed and only form in a small region of the SiC layer.

Both elastic mechanical compressive stresses (dark spots) and Moire patterns formed due to the superposition of two disoriented crystal lattice Si (highlighted in the drawing by the green region) are observed in silicon in the image closer to the interface. The diffraction pattern (Figure 2, *d*) shows the so-called „double diffraction“, which results in the formation of additional reflexes around the main Si reflexes (in Figure 2, *d* this diffraction is indicated by green arrows). A „triple periodicity“ is observed in two directions in a SiC layer: parallel to the surface (blue region) and at an angle 54.75° (white region). These are areas with weakly intense reflexes in the diffraction pattern (Figure 2, *d*), they are indicative of twinning of the underlying matrix. They are indicated by white and blue arrows in Figure 2, *d*, respectively.

When the synthesis time is further increased, the structure of the SiC/Si interface undergoes significant changes (Figure 3). Phases with triple periodicity in the $\langle 110 \rangle$ direction are hardly observed at the interface of the sample SiC/Si-3*n* (Figure 3, *a*). At the same time, twins appeared in the $\langle 100 \rangle$ direction, both in the SiC layer and in the Si substrate. On the contrary, the beginning of twin structure formation along the $\langle 110 \rangle$ direction can be seen in the interfacial zone in SiC/Si-3*p* sample. Moreover, the formation of these structures occurs already in the silicon substrate itself, far from the interfacial boundary. Twin formation is particularly intense in the SiC layer of the SiC/Si-3*n* sample along the $\langle 100 \rangle$ direction. In silicon itself, there are significant changes in its crystal lattice, as evidenced by the Moire pattern, which goes deeper into

the Si layer; accordingly, the diffraction pattern (Figure 3, *b*) shows bright reflexes from the „double diffraction“, located around the main reflexes of Si (they are indicated by green circles in Figure 3, *b*). Reflections from „double diffraction“ are also observed around the main SiC reflexes, but they are less intense. These reflexes are formed from a layer with a Moire pattern. A possible reason for the formation of this Moire pattern— is the superimposition of a layer of Si of a different orientation on the SiC layer. The „triple periodicity“ is also observed in the SiC layer, but it is oriented at an angle of 54.75° , and there is almost no „triple periodicity“ parallel to the SiC/Si interface.

An even more complex Moire pattern is observed in the SiC/Si-3*p* sample, where several Si directions overlap. This disruption of the crystal structure of the substrate goes deeper into the Si layer and begins to appear in the pore neighborhood and reaches the Si/SiC interface. The electron diffraction image was obtained using „selective aperture“ (the selection region is shown by the blue circle in the SEM image, thus we got rid of unnecessary „double diffraction“ reflexes). We see streaks along the SiC reflexes on the diffraction. They are oriented only in one direction and, correspond to stacking faults oriented at an angle 54.75° to the interface. Reflexes from twinning of the corresponding „triple periodicity“ in the same direction are observed on the streaks.

The inversion of the structure of the SiC/Si interface takes place after 40 min of synthesis (Figure 4). There are no phases with triple periodicity in the SiC/Si-40*n* sample (Figure 4, *a*), but twins oriented at an angle 54.75° in the $\langle 100 \rangle$ directions are clearly visible. Twin reflexes from „triple periodicity“ (white arrows in drawing 4, *b*) are visible in the electron diffraction image in addition to the main SiC reflexes, as well as streaks that correspond to stacking faults, all oriented at an angle 54.75° to the interface.

The SiC/Si-40*p* sample (Figure 4, *c*) has a fundamentally different structure. It practically replicates the structure of the SiC sample grown on the Si substrate of *n*-type during 1 min of synthesis. The formation of twin layers with a period equal to 0.252 nm can be traced in this sample, as in the sample whose image is shown in Figure 2, *a*, and every three layers this structure is repeated (orange arrows indicate these defects). The distance between layer repetitions is 0.756 nm. The Figure also shows stacking faults directed at an angle 54.75° to the interface (they are labeled with white lines); however, diffraction reflections from them are barely visible.

5. Discussion of results

We noted above that the structure studies performed in Ref. [3] could not provide a definite answer about the physical reasons leading to such different magnetic susceptibility time dependencies of synthesized SiC/Si samples on Si substrates of *n*- and *p*-type of conductivity. Only by studying

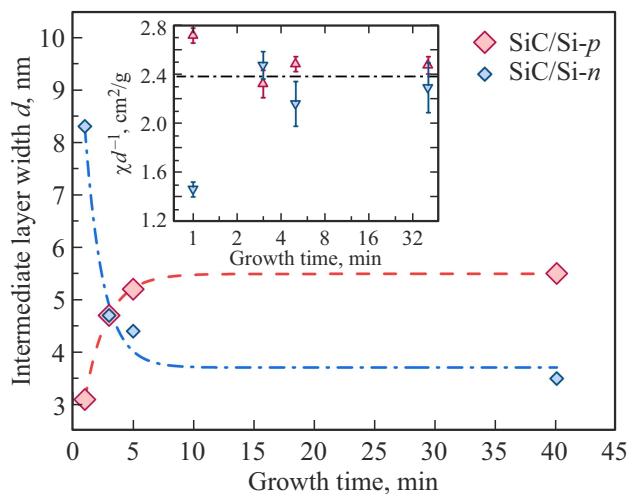


Figure 5. The dependences of the twin layers thickness, obtained from TEM data (Figures 2–4).

the evolution of the microstructure of these samples by HP TEM, we were able to detect fundamental differences in the interface structure in SiC/Si samples grown on Si substrates of n -type and p -type of conductivity at different synthesis times. Analysis of TEM images unambiguously showed that twin regions of silicon carbide of the 3C-SiC polytype with a period equal to 0.252 nm with a triple periodicity with an interval of 0.756 nm are formed at the SiC-Si interface in the samples that possess the maximum, in absolute value, value of magnetic susceptibility, i.e. every three layers they are repeated. Moreover, these regions are observed along the (111) plane, practically along the entire length of the sample, and their number is of the order of ten. In result, the thickness of the entire transition layer containing the twin regions of silicon carbide can reach values on the order of 10–11 nm. There is either no such a structure in samples, which have a smaller absolute value of magnetic susceptibility or the thickness of this layer is much smaller, of the order of 1–3 nm. We emphasize again that the thickness is determined by the number of silicon carbide twin layers. In addition, twin layers with thicknesses on the order of 1–10 nm are also formed in these samples, but they are oriented not along the $\langle 111 \rangle$ direction, but along the $\langle 100 \rangle$ direction. These data are fully correlated with the magnetic susceptibility measurements (Figure 1). In our opinion, this indicates, first, that the SiC/Si samples have significantly greater diamagnetic properties than silicon and silicon carbide individually, and second, that the diamagnetism of SiC/Si is determined mainly by the structure and thickness of the SiC-Si transition layer. Figure 5 shows the dependences of the values of the thicknesses, determined by the thickness of the twin layers, of the transition layer of SiC/Si samples on the synthesis time, plotted from the data obtained by HR TEM, whose images are shown in Figures 2–4. It can be seen from the graphs shown in Figure 5 that the thickness dependences

of the transition layers behave similarly to the magnetic susceptibility dependences shown in Figure 1. These results, in our opinion, unequivocally prove that it is the discussed physical properties of the transition layer between 3C-SiC and Si that are responsible for the detected anomaly in the magnetic properties of the hybrid structures.

Figure 6, *a* shows the structure of SiC twin interfacial layers (i.e. the boundary between 3C-SiC (111) and 3C-SiC ($\bar{1}\bar{1}\bar{1}$)), in which the carbon atoms are opposite each other, resulting in the formation of C–C bonds with the length of 1.6 Å. This structure is calculated by the density functional method in the Medea-Vasp package using pseudopotentials and plane waves with a cutoff energy of 400 eV. The calculations show that this twinning boundary attracts silicon vacancies on both the silicon and silicon carbide sides, thereby lowering the total energy of the system by about 3.5 eV per vacancy. Just as in the volume, silicon vacancies are attracted to each other in the $\langle 1\bar{1}0 \rangle$ direction, forming vacancy filaments in this direction [16]. Figure 6, *b* shows an image of the twin structure with a vacancy thread in the $\langle 1\bar{1}0 \rangle$ direction (i.e., silicon atoms are absent in every other position in this direction [16]). Density functional calculations show that there is no magnetic moment in the initial state as well as in the SiC volume. However, such a state is metastable. Calculations have shown that it is advantageous for the electron of the carbon atom above the vacancy strand to tunnel to another carbon atom to the right of the vacancy (Figure 6, *b*) at a distance 3.4 Å. This probability is approximately 40%. In this case, the spin of the electron necessarily reverses its direction. The result is that the system acquires a magnetic moment of 0.8 Bohr magneton and energy of about 0.01 eV

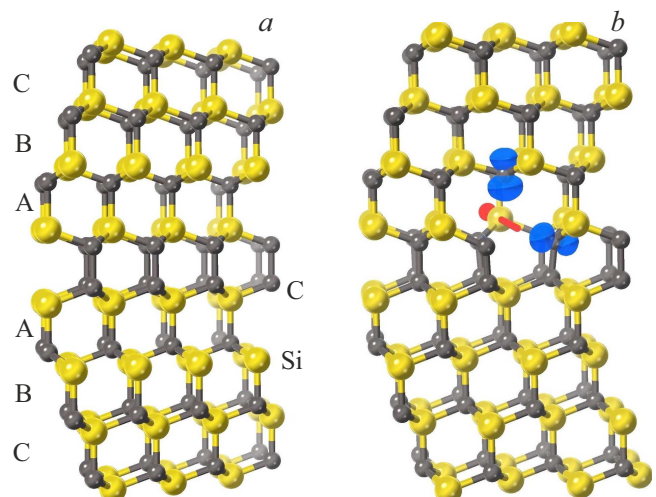


Figure 6. (*a*) Image of twinning boundary in 3C-SiC with C–C bonds. The positions of densely stacked layers in 3C-SiC are denoted by A, B, C; (*b*) Doubling boundary in 3C-SiC with silicon vacancy filament in the $\langle 1\bar{1}0 \rangle$ direction marked by the red arrow. The regions of magnetic moment of 0.04 electron at Å³, i.e. difference in density of electrons with spin up and spin down, are marked by blue color.

is released, corresponding to a radiation frequency of 2.4 THz. The region with a magnetic moment greater than 0.04 electrons on \AA^3 is shown in Figure 6, *b* in blue.

The measured susceptibility values were calculated per unit weight of the samples for the determination of magnetic susceptibility. The results of the microstructure analysis obtained by HR TEM showed that out of the whole sample weight, only the transition layer is the main contributor to the magnetic susceptibility. This fact unambiguously indicates that it is necessary, based on the data obtained by the HR TEM method, to recalculate the value of the magnetic susceptibility of the hybrid structure, given in Figure 1, as applied only to the transition layer.

The thicknesses of the SiC layers and the values of the thicknesses of the silicon bed underneath the SiC layer can be determined with a reasonable degree of accuracy from the TEM data. Comparing these thicknesses with the thicknesses of SiC layers obtained by ellipsometry, given in Ref. [3] (as indicated above, the data on magnetic susceptibility, presented in Figure 1, obtained from the same samples [3]) it is possible to show that they almost coincide, which, however, is to be expected. We provided the values of the silicon magnetic susceptibility of $\chi(T, H) = -0.228 \cdot 10^{-6} \text{ cm}^3/\text{g}$ and the silicon carbide magnetic susceptibility of $\chi(T, H) = -0.265 \cdot 10^{-6} \text{ cm}^3/\text{g}$ at 300 K in the introduction. Thus, the magnetic susceptibility values of silicon carbide and silicon are of the same order. Since the thickness of the silicon substrate equal to $400 \mu\text{m}$ is more than 80–100 times larger than the thicknesses of the SiC layers lying in the region of 40–65 nm (see Figure 7 in Ref. [3]), then with a high degree of accuracy, it can be stated that the magnetic susceptibility of the Si substrate with a SiC layer, without a transition layer, has an average value that coincides with the magnetic susceptibility of silicon, i.e., it has a value of the order of $\chi(T, H) \cong -0.23 \cdot 10^{-6} \text{ cm}^3/\text{g}$. It follows from the data in Figure 1 that our measured values of the magnetic susceptibility of the SiC/Si samples lie in the region of values from

$$\chi(T, H) \sim -(0.8 \div 1.4) \cdot 10^{-6} \text{ cm}^3/\text{g}.$$

If we subtract the value $\chi(T, H) \sim -0.2 \cdot 10^{-6} \text{ cm}^3/\text{g}$ from the magnetic susceptibility values shown in Figure 1, and consider that the density of Si is 2.3 g/cm^3 , and the density of 3C-SiC is 3.2 g/cm^3 [17], then we obtain that the magnetic susceptibilities of the transition layers per total mass of SiC/Si samples, i.e., per mass of both silicon and silicon carbide lie in the region of values

$$\chi(T, H) \sim -(0.6 \div 1.2) \cdot 10^{-6} \text{ cm}^3/\text{g}.$$

The thickness of the transition layer varies from 10 nm for SiC layers grown on Si substrate of *n*-type for 1 min and SiC layers grown on Si substrate of *p*-type for 40 min to a thickness of the order of 1 nm and less for SiC layers grown on Si substrate of *p*-type for 1 min and Si substrate of *n*-type for 40 min. Since the transition layers are SiC twins, the

density of the transition layer can be put equal to that of SiC. It follows that approximately in terms of the mass of a one nanometer thick layer, its magnetic susceptibility is of the order of magnitude $\chi(T, H) \sim -5 \cdot 10^{-4} \text{ cm}^3/\text{g}$ or, given the density of SiC, in dimensionless form $\chi(T, H) \sim -2 \cdot 10^{-3}$. This value of magnetic susceptibility, taken modulo the absolute values of magnetic susceptibility of most carbon structures [12]. A more precise value for this value is not yet possible because more accurate data on the size of the SiC-Si transition regions are needed. However, the magnetic susceptibility value we found differs significantly from both the magnetic susceptibility values of silicon and silicon carbide and the magnetic susceptibility values of various carbon structures. This suggests that the transition state at the SiC/Si interface is a new, previously unknown nanostructure formed on Si during the synthesis of SiC by the coordinated atom substitution method [4,5].

In our opinion, the phenomenon of the generation of intrinsic terahertz radiation (THz) in the frequency range of 0.12 THz and 3.4 THz from SiC/Si nanostructures, which we discovered earlier [18,19], is attributable to the formation of a special kind of twin layers with a period equal to 0.252 nm and with a triple periodicity with an interval of 0.756 nm (Figures 2–4) and with an ensemble of silicon vacancies located in the twin boundary region (Figure 6, *b*).

It should be noted that the detected effect of the formation of a special structure of the interfacial interface during the chemical synthesis of SiC is obviously inherent in a wide class of solid-phase chemical transformations. Thus, the formation of transition phases of the PdSe_{2-x} type was found in Ref. [20] during the synthesis of ultrathin films of palladium selenite (PdSe_2), the composition, structure, and electrical properties of which were a function of synthesis time PdSe_2 .

6. Conclusions

As a result of the study conducted in this paper, the dependences of magnetic susceptibility on the time of synthesis of SiC from Si using the method of coordinated atomic substitution were obtained. The following was found.

- The magnetic susceptibility of all, without exception, SiC/Si samples is diamagnetic, i.e. all SiC/Si hybrid structures are diamagnetic.
- The absolute value of magnetic susceptibility at room temperature, anomalously, is more than three orders of magnitude higher than the magnetic susceptibility values of diamagnetics such as silicon and silicon carbide.
- The absolute value of magnetic susceptibility at room temperature is an order of magnitude greater than the same characteristic of highly oriented pyrolytic graphite (HOPG).
- The microscopic studies by HR TEM of the SiC/Si interface of samples whose magnetic susceptibility was measured by the Faraday method proved that the main contribution to the diamagnetism of the hybrid structure comes from the SiC-Si transition. This layer consists of

twinned, ordered layers arranged parallel to the interface boundary in the plane (111) with a period equal to 0.252 nm with a triple periodicity with an interval of 0.756 nm, i.e., every three layers are repeated.

– The magnetic susceptibility of each twin layer has a value approximately equal to $\chi(T, H) \sim -5 \cdot 10^{-4} \text{ cm}^3/\text{g}$.

– The number of twin layers varies depending on the time of growth of the SiC layer on Si(111). Moreover, this number varies antisymmetrically in case of SiC layers grown on Si substrates of *n*- and *p*-types of conductivity. At the beginning of the process of growing (synthesis during the 1st minute) of SiC on Si substrate of *n*-type of conductivity, the number of twin layers is larger than that on Si substrate of *p*-type of conductivity, whereas at the completion of 40-min synthesis, the density of these layers is significantly higher on the Si substrate of *p*-type of conductivity than on the Si substrate of *n*-type of conductivity.

– Quantum mechanical calculations have shown that the interfacial boundary region with twin layer structure is an attractor for silicon vacancies.

Funding

This work was performed with funding from an R&D pilot project of the Russian Science Foundation No. 23-91-01001.

Acknowledgments

The SiC structures were grown on Si w using the equipment of the unique research facility „Physics, Chemistry and Mechanics of Crystals and Thin Films“ of FSUE Institute for Problems in Mechanical Engineering of the Russian Academy of Sciences (St.Petersburg), magnetic susceptibility measurements were carried out at the Department of Physics of Peter the Great St.Petersburg Polytechnic University, and TEM studies were conducted using the equipment of „Nanotechnologies“ International Research Center of the St.Petersburg State University.

The authors are sincerely grateful to M.G. Vorobyov and A.S. Grashchenko for their help in synthesizing SiC on Si layers.

Conflict of interest

The authors declare that they have no conflict of interest.

References

- [1] S.A. Kukushkin, A.V. Osipov, E.V. Osipova, V.M. Stozharov. *PSS* **64**, 3, 327 (2022). DOI: 10.21883/PSS.2022.03.53187.232
- [2] I.A. Eremeev, M.G. Vorobev, A.S. Grashchenko, A.V. Semench, A.V. Osipov, S.A. Kukushkin. *PSS* **65**, 1, 68 (2023). DOI: 10.21883/PSS.2023.01.54976.480
- [3] S.A. Kukushkin¹, M.G. Vorobev, A.V. Osipov, A.S. Grashchenko, E.V. Ubyivovk. *PSS* **66**, 7, 1094 (2023). DOI: 10.61011/PSS.2024.07.58982.120
- [4] S.A. Kukushkin, A.V. Osipov. *Russian Journal of Gen. Chem.* **92**, 4, 547 (2022). DOI: 10.1134/S1070363222040028).
- [5] S.A. Kukushkin, A.V. Osipov. *Condensed Matter and Interphases* **24**, 4, 407 (2022). DOI: 10.17308/kcmf.2022.24/10549
- [6] A. Severino, C. Locke, R. Anzalone, M. Camarda, N. Piluso, A. La Magna, S. Sadow, G. Abbondanza, G. D'Arrigo, F. La Via. *ECS Trans* **35**, 6, 99 (2011). DOI: 10.1149/1.3570851
- [7] G. Ferro. *Crit. Rev. Solid State Mater. Sci.* **40**, 1, 56 (2015). DOI: 10.1080/10408436.2014.940440
- [8] S. Nishino, J.A. Powell, H.A. Will. *Appl. Phys. Lett.* **42**, 5, 460 (1983). DOI: 10.1063/1.93970
- [9] N.T. Bagraev, S.A. Kukushkin, A.V. Osipov, V.V. Romanov, L.E. Klyachkin, A.M. Malyarenko, V.S. Khromov. *Semiconductors* **55**, 2, 37 (2021). DOI: 10.1134/S106378262102007X
- [10] I.K. Kikoin. *Tablitsy fizicheskikh velichin: Spravochnik*. Publisher: Atomizdat. (1976) p. 1008. (in Russian).
- [11] I.P. Kalinkin, S.A. Kukushkin, A.V. Osipov. *Semiconductors* **52**, 802 (2018). DOI: 10.1134/S1063782618060118
- [12] T.L. Makarova. *FTP* **38**, 6, 641 (2004). (in Russian).
- [13] S.A. Kukushkin, A.V. Osipov. *Materials* **14**, 1, 78 (2021). <https://doi.org/10.3390/ma14010078>
- [14] S.A. Kukushkin, A.V. Osipov. *Pisma v ZhTF* **46**, 22, 3 (2020). (in Russian). <https://doi.org/10.21883/PJTF.2020.22.50298.18439>
- [15] U. Kaiser, A. Chuvilin, P.D. Brown, W. Richter. *Microsc. Microanal.* **5**, 420 (1999). DOI: 10.1017/S1431927699990487
- [16] S.A. Kukushkin, A.V. Osipov. *Pisma v ZhTF* **50**, 21, 19 (2024). (in Russian). DOI: 10.61011/PJTF.2024.21.58953.20027
- [17] S.A. Kukushkin, A.V. Osipov, V.N. Bessolov, B.K. Medvedev, V.K. Nevolin, K.A. Tcarik. *Rev. Adv. Mater. Sci.* **17**, 1/2, 1 (2008). https://www.ipme.ru/e-journals/RAMS/no_11708/kukushkin.pdf
- [18] N.T. Bagraev, S.A. Kukushkin, A.V. Osipov, L.E. Klyachkin, A.M. Malyarenko, V.S. Khromov. *FTP* **55**, 11, 1027 (2021). (in Russian). DOI: 10.21883/FTP.2021.11.51556.9709
- [19] N.T. Bagraev, S.A. Kukushkin, A.V. Osipov, L.E. Klyachkin, A.M. Malyarenko, V.S. Khromov. *FTP* **55**, 12, 1195 (2021). (in Russian). DOI: 10.21883/FTP.2021.12.51705.9620
- [20] R. Zhang, Q. Zhang, X. Jia, S. Wen, H. Wu, Y. Gong, Y. In, C. Lan, C. Li. *Nanotechnology* **34**, 34, 345704 (2023). DOI: 10.1088/1361-6528/acd855

Translated by A.Akhtyamov